ii) compute the Fourier transform of the sequence $(1, \varrho_1^L, \cdots, \varrho_{n-1}^L)$, thus determining matrices C and Π (cf. (11) and (12));
iii) compute the residues at the above poles and find the values of b_{mk} using (18);
iv) determine the components of the output vector A as partitioned in (14) by inverse Fourier transformation:

$$a_{mj} = \frac{1}{n}\sum_{k=1}^{n-1} b_{mk}\, e^{j2\pi kj/n}, \qquad m = 1, 2, \cdots, L, \quad j = 0, 1, \cdots, n-1. \tag{21}$$

V. Example

Let us consider the synthesis of a spectral density (20) with $n = 4$, $\varrho_1 = (1+i)/3$, $\varrho_2 = 1/2$, $\varrho_3 = (1-i)/3$ and positive values of the ratios r_k/ϱ_k. As it can easily be verified, the discrete Fourier transform (11) of $[1, \varrho_1, \varrho_2, \varrho_3]$ leads to a circulant matrix with some negative entries. However, according to Corollary 1 with $L = 2$, there exists a circulant stochastic matrix C with the eigenvalues 1, $\varrho_1^2 = 2i/9$, $\varrho_2^2 = 1/4$, $\varrho_3^2 = -2i/9$. From (11), the entries of the first row of this circulant matrix turn out to be

$$\frac{1}{144}[45 \quad 11 \quad 45 \quad 43].$$

This enables us to find the transition probability matrix Π as in (12) with $L = 2$. In this way, the resulting SM has $nL = 8$ states. The output vector A can finally be obtained through (18) and (21).

References

[1] J. L. Doob, *Stochastic Processes*. New York: Wiley, 1953.
[2] C. T. Mullis and R. A. Roberts, "On weak equivalence of linear systems and finite state systems," *SIAM J. Math. Anal.*, vol. 10, no. 3, pp. 498–511, 1979.
[3] C. T. Mullis and K. Steiglitz, "Circulant Markov chains as digital signal sources," *IEEE Trans. Audio Electroacoust.*, vol. AU-20, no. 4, pp. 246–248, 1972.
[4] Z. Kohavi, *Switching and Finite Automata Theory*. New York: McGraw-Hill, 1970.
[5] A. Paz, *Introduction to Probabilistic Automata*. New York: Academic, 1977.
[6] J. G. Kemeny and J. L. Snell, *Finite Markov Chains*. New York: Van Nostrand, 1960.
[7] P. Lancaster, *Theory of Matrices*. New York: Academic, 1969.
[8] G. Bilardi, R. Padovani, and G. L. Pierobon, "Spectral analysis of functions of Markov chains with applications," *IEEE Trans. Commun.*, vol. COM-31, no. 7, pp. 853–861, 1983.
[9] C. M. Monti and G. L. Pierobon, "Circulant stochastic matrices with assigned eigenvalues," Dep. Electron. Informatics, Int. Rep., Univ. Padova, 1991.

Kernel Design for Time-Frequency Signal Analysis Using the Radon Transform

Branko Ristic and Boualem Boashash

***Abstract*—This correspondence presents a new kernel design technique for time-frequency signal analysis. The technique is based on the Radon transform of the modulus of the ambiguity function of the signal for determination of the angles and distances of the radially distributed contents of the autoterms in the ambiguity domain. The proposed kernel effectively reduces the cross-terms and noise for linear FM signals. The result is a tool for high-resolution time-frequency representation of nonstationary, primarily linear FM signals.**

Manuscript received December 5, 1991; revised June 29, 1992. The associate editor coordinating the review of this correspondence and approving it for publication was Prof. Miguel A. Lagunas. This work was supported by the Defence Science and Technology Organisation, Australia and the Australian Research Council.

The authors are with the Signal Processing Research Centre, Queensland University of Technology, Brisbane, Q.4001 Australia.

IEEE Log Number 9207544.

I. Introduction

Any bilinear time-frequency distribution (TFD) can be expressed as the two-dimensional Fourier transform of the product of the symmetrical ambiguity function of the signal (in text referred to as the ambiguity function, AF) and the kernel $\varphi(\theta, \tau)$ [7]:

$$P_z(t, f) = \int_{-\infty}^{\infty}\int_{-\infty}^{\infty} A_z(\theta, \tau)\varphi(\theta, \tau) e^{j2\pi\theta t} e^{-j2\pi f\tau}\, d\theta\, d\tau \tag{1}$$

where the ambiguity function $A_z(\theta, \tau)$ is defined as [7]

$$A_z(\theta, \tau) = \int_{-\infty}^{\infty} z(t + \tau/2)\cdot z^*(t - \tau/2) e^{j2\pi\theta t}\, dt. \tag{2}$$

A number of kernels were proposed [2], [7] in order to suppress the influence of the artifacts and noise. Some of them are fixed (signal independent) [5], [13] the others are adaptively designed for the signal under analysis (signal dependent) [1], [10]. Only the signal independent kernel based TFD's can preserve the desirable properties of the WVD [6]. However, since the kernel function is actually the transfer function of a two-dimensional filter (dimensions are θ and τ), for suppression of artifacts and noise, the kernel design (as the filter design) has to be signal dependent in order to obtain good performance for a broader class of signals.

The problem addressed in this correspondence is a signal dependent kernel design for time-frequency signal analysis. In a variety of publications on the subject it is important to mention the work by Baraniuk and Jones [1] who treated the kernel design as an optimization problem. In this correspondence we propose a simpler approach based on the Radon transform of the modulus of the AF.

II. Theoretical Consideration for Linear FM Signal Components

A. Background

We model each signal segment as

$$z(t) = \sum_{k=1}^{K} z_k(t) + n(t), \qquad (0 \le t \le T)$$

where K is the number of signal components of $z(t)$, $n(t)$ is the noise, and T is the segment duration. We further model each component as a finite duration unit amplitude quadratic phase signal:

$$z_k(t) = e^{j\phi_k(t)} = \exp\left\{j2\pi\left(a_{0k} + a_{1k}t + \frac{a_{2k}}{2}t^2\right)\right\}$$
$$0 \le t_{0k} \le t \le t_{0k} + T_k \le T. \tag{3}$$

The signal component k starts at t_{0k} and exists during the period T_k. For simplification, unit amplitudes are assumed. In case the signal components have arbitrary constant amplitudes, only step 2 of the kernel design procedure will change (Section III). From the definition of the instantaneous frequency of a signal component, $f_k(t) = (1/2\pi)(d\phi_k(t)/dt)$ we get

$$f_k(t) = a_{1k} + a_{2k}t \qquad 0 \le t_{0k} \le t \le t_{0k} + T_k \le T. \tag{4}$$

In our model we assume a linear change of frequency for each component in the signal segment, since we can satisfy this assumption by choosing the segment duration T to be sufficiently small. (Notice, however, that with smaller T, the noise performance and the frequency resolution become worse [3].) The bilinear product of the WVD is given by

$$q_z(t, \tau) = z(t + \tau/2)z^*(t - \tau/2) = \sum_{k=1}^{K} \exp\{j 2\pi(a_{1k} + a_{2k}t)\} + \xi_K(t, \tau) \quad (5)$$

where $-t \le \tau \le t$ for $0 \le t \le T/2$ and $t - T \le \tau \le -(t - T)$ for $T/2 \le t \le T$. The coefficients a_{2k} are referred to as the frequency rate coefficients. The term $\xi_K(t, \tau)$ in (5) denotes the influence of the artifacts and noise. Our aim is to filter out this influence in an automatic way. The best choice of the signal analysis domain in which the filtering should be done is the Doppler (θ) − lag (τ) domain (ambiguity domain) for two reasons: i) In the ambiguity domain, the filtering is performed by multiplication of the AF and the kernel rather than by double convolution of the WVD and the 2D Fourier transform of the kernel [2]; ii) The autoterms are known to pass through the origin of the (θ, τ), as will be shown latter.

The ambiguity function of the signal $z(t)$, assuming infinite duration of signal and each of its components $T_k \to \infty$ for $k = 1, 2, \cdots, K$ is

$$A_z(\theta, \tau) = \mathop{\mathcal{F}}_{t \to \theta}[q(t, \tau)] = \sum_{k=1}^{K} e^{j 2\pi a_{1k}\tau}\delta(\theta - \tau a_{2k}) + \mathop{\mathcal{F}}_{t \to \theta}\{\xi_K(t, \tau)\}. \quad (6)$$

From (6) we observe that the autoterms represent straight lines of complex valued delta impulses in the (θ, τ) plane. Cross-terms have oscillatory amplitude and therefore they appear at a distance from the origin, the distance being in direct relation to the time-frequency distance between the signal components [8]. The stationary noise appears only along the τ axis in the ambiguity domain. In kernel design we use the modulus of the AF in order to estimate the angles of significant radial content in (θ, τ) plane. The modulus of the AF can be expressed as

$$|A_z(\theta, \tau)| = \sum_{k=1}^{K} \delta(\theta - \tau a_{2k}) + \Xi_K(\theta, \tau). \quad (7)$$

The first term on the RHS of (7) describes the modulus of the AF in a hypothetical case where cross-terms do not exist and the noise power is zero (i.e., $\Xi_K(\theta, \tau) = 0$). In real situations $\Xi_K(\theta, \tau)$ is a two-dimensional function which consists of a deterministic part (signal cross-terms) and a random part (noise and the signal-noise cross-terms). Based on the locations of the cross-terms and noise we know that $\Xi_K(\theta, \tau)$ does not lend itself to the structure of the first term on the RHS of (7) and it does not represent lines going through the origin of the (θ, τ) plane. This simple observation is crucial for the discussion that follows in this section.

B. Problem Definition

Consider the modulus of the AF of a signal consisting of K linear FM components. Since $|A_z(\theta, \tau)|$ given by (7) can be interpreted as a set of lines in the (θ, τ) plane traversing the origin, the first problem is to estimate the angles $\phi_k = \arctan a_{2k}$ composed by those lines (that corresponding to signal components) and the τ axis. For $T_k \to \infty$ ($k = 1, \cdots, K$) this would be all that has to be done. However, in practice, T_k's and consequently lengths of radial lines representing the components in the ambiguity domain are finite. Therefore, the additional problem is to estimate radial distances for each signal component. This is illustrated in Fig. 1 for case $K = 2$. The problem becomes complicated if the number of components K is unknown or if the frequency rate coefficients of some of the components are equal (i.e., $\exists i, j$ such that $i \ne j$ and $a_{2i} = a_{2j}$).

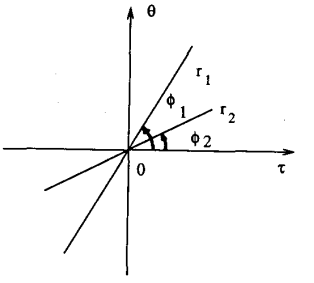

Fig. 1. Two signal components in the (θ, τ) plane.

C. The Radon Transform as a Tool

It is very convenient to analyze the function $|A_z(\theta, \tau)|$ as given by (7) using the Radon transform (RT) [12]. The Radon transform has been used in image analysis, particularly in image reconstruction from projections. When applied to a two-dimensional function $f(x, y)$ it represents the sum of the values of $f(x,y)$ along the line at distance s from the origin, and at angle ϕ with the x axis [9]:

$$\mathcal{R}_{s,\phi}\{f(x, y)\} = \int_{-\infty}^{\infty}\int_{-\infty}^{\infty} f(x, y) \cdot \delta(x \sin\phi + y \cos\phi - s)\, dx\, dy \quad (8)$$

for $-\infty < s < \infty$ and $(-\pi/2) < \phi < (\pi/2)$, where $\mathcal{R}_{s,\phi}\{\ \}$ is the Radon transform.

Thus, applying the RT at distance $s = 0$ to the function $|A_z(\theta, \tau)|$ as given by (7) we obtain

$$R_0(\phi) = \mathcal{R}_{s,\phi}\{|A_z(\theta, \tau)|\}|_{s=0} \quad (9)$$

$$= \sum_{k=1}^{K} \gamma_k \delta(\phi - \arctan a_{2k}) + \chi_K(\phi) \quad (10)$$

for $-\pi/2 < \phi < \pi/2$ and $T_k \to \infty$, where γ_k denotes the length of the radial line in the (θ, τ) plane, and theoretically tends to infinity as $T_k \to \infty$. Integrating along the lines through the origin of the ambiguity domain, the RT efficiently detects the autoterms, since the autoterms also represent the lines going through the origin, while the cross-terms and the noise terms do not. Consequently, the values of $\chi_K(\phi) = \mathcal{R}_{s,\phi}\{\Xi_K(\theta, \tau)\}|_{s=0}$ will be less than $\gamma_k\delta(0)$ for all k, assuming high SNR.

In order to illustrate the above equations, consider a signal consisting of two components, with instantaneous frequencies shown in Fig. 2. In Fig. 3 the WVD of the signal is given (only positive values are shown). Figs. 4 and 5 present the modulus of the AF of the signal and its Radon transform at $s = 0$, respectively. Two sharp peaks in $R_0(\phi)$ correspond to the autoterms.

III. Kernel Design Procedure

The kernel design procedure consists of three steps:

Step 1: Estimation of angles ϕ of significant radial contents. This step is based on (10) and is performed by finding the local

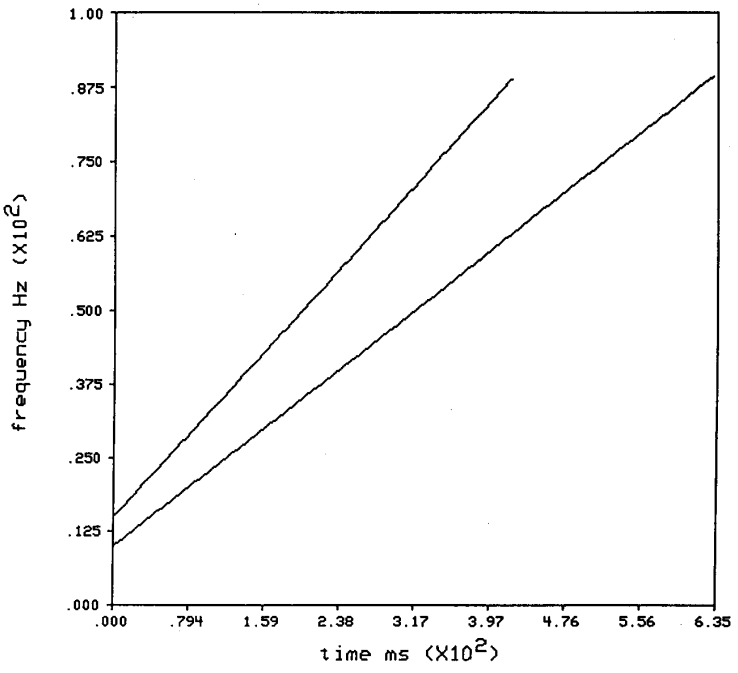

Fig. 2. Instantaneous frequencies of signal A consisting of two linear FM components.

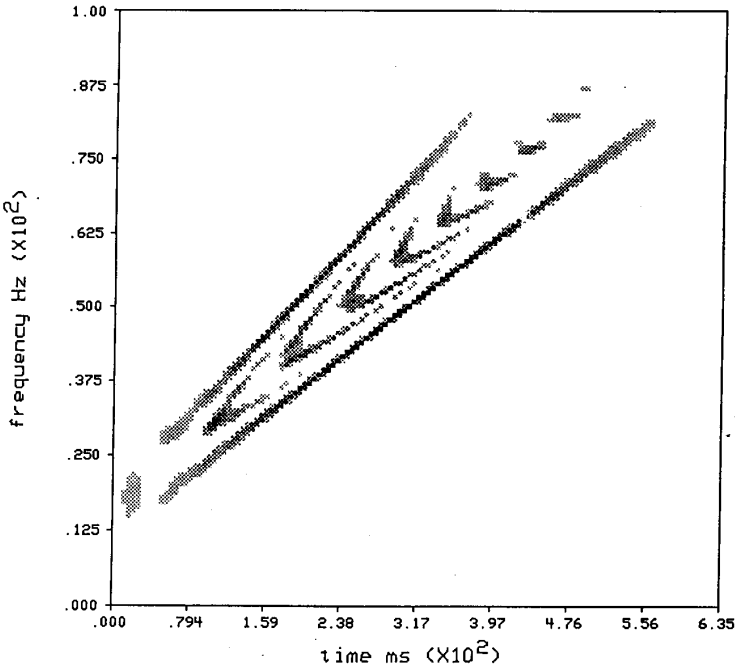

Fig. 3. Wigner–Ville distribution of signal A.

maxima of the function $R_0(\phi)$. We can distinguish two possible cases:

Case 1: When the number of components K is known and the frequency rate coefficients of components are all mutually different: $a_{2i} \neq a_{2j}$; $(i \neq j, i, j = 1, \cdots, K)$, the procedure is to apply the peak searching algorithm to $R_0(\phi)$ and to find K values of the set:

$$\Phi_K = \{\phi : \phi = \arctan a_{2k};\ k = 1, 2, \cdots, K\}.$$

Case 2: When no *a priori* information is available, one can introduce an alternative parameter β (or b) that controls the tradeoff

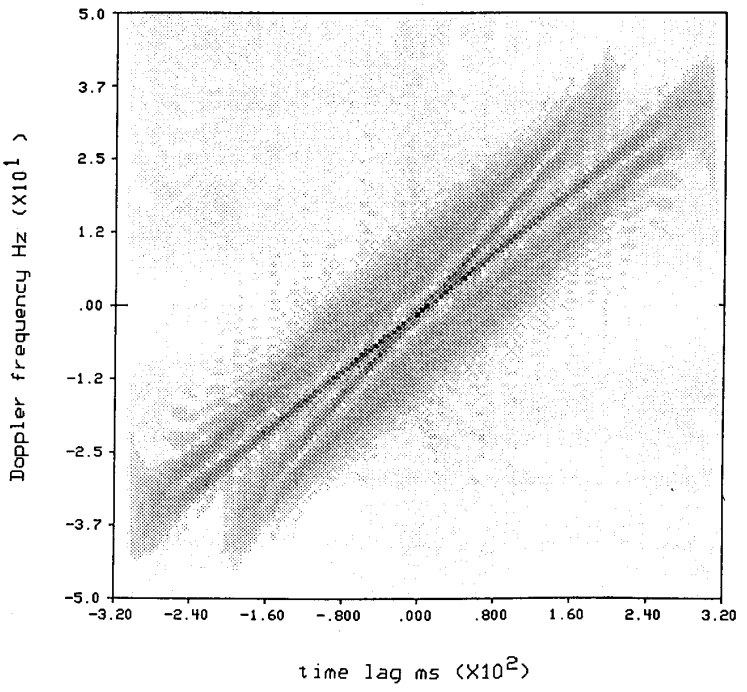

Fig. 4. The modulus of the ambiguity function of signal A.

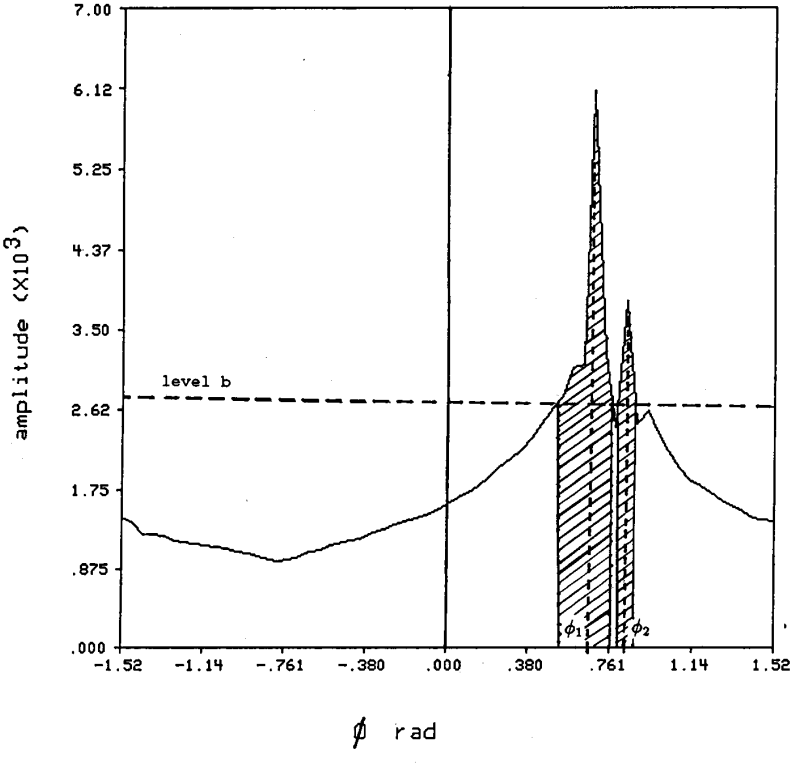

Fig. 5. Radon transform at $s = 0$ of the modulus of the AF of signal A.

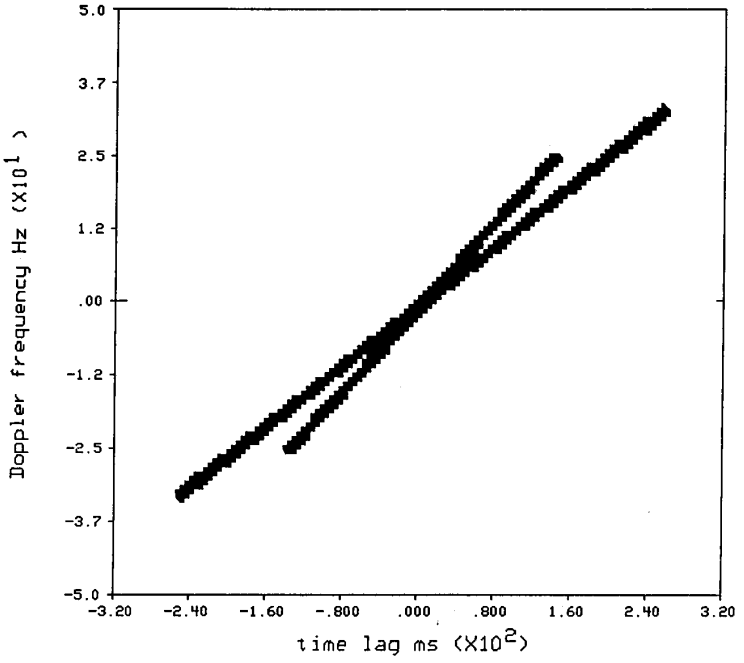

Fig. 6. Kernel designed for signal A ($K = 2$ or beta = 0.02 and ϵ 0.1).

between the cross-component suppression and autocomponent smoothing. This tradeoff can be expressed by the ratio:

$$\beta = \frac{\int_{-\pi/2}^{\pi/2} R_{0b}(\phi)\, d\phi}{\int_{-\pi/2}^{\pi/2} R_0(\phi)\, d\phi} \tag{11}$$

where

$$R_{0b}(\phi) = \begin{cases} 0 & \text{if } R_0(\phi) < b \\ R_0(\phi) - b & \text{if } R_0(\phi) \geq b \end{cases}$$

(notice that b and β are a single parameter, since knowing one of them we can calculate the other). The β parameter is defined as the ratio of the area under the function $R_0(\phi)$ above the level b (Fig. 5), and the total area under the $R_0(\phi)$. It controls what portion of the signal energy will pass through the two-dimensional kernel filter. This portion is shown by the shaded area in Fig. 5. Small values of β suppress the cross-terms and the noise, but if β is too small, it may also filter out some of the autoterm energy. The definition limits β to values less than or equal to 1, and in simulations we typically use $\beta < 0.1$.

The procedure for the step 1 is to find the set of intervals of ϕ for which $R_{0b}(\phi) > 0$:

$$\Phi_b = \{\phi : R_{0b}(\phi) > 0\} \equiv \{\phi : R_0(\phi) > b\}.$$

Step 2: Estimation of distance r of the significant radial contents.

Distances of radial content are estimated only at angles ϕ that are found by the step 1. They are proportional to the value $R_0(\phi)$ as it can be seen from (7) if we neglect $\Xi_K(\theta, \tau)$. Thus we estimate a subset of all distances r

$$\rho_{K/b} = \left\{ r : r = \frac{r_m}{R_0(\phi_m)} \times R_0(\phi); \quad \phi \in \Phi_{K/b} \right\} \tag{12}$$

where the subscript K/b indicates the case in step 1; ϕ_m is the modal value of $R_0(\phi)$, that is $R_0(\phi_m) \geq R_0(\phi)$ for $-\pi/2 < \phi < \pi/2$; r_m is the maximum value of r such that $|A_z(r, \phi)| > \epsilon |A_z(0, 0)|$ where $A_z(r, \phi)$ is the AF in polar coordinates, $|A_z(0, 0)| \geq |A_z(\theta, \tau)|$, and ϵ is the parameter that controls the radial distance of the component that produces the global maximum of the $R_0(\phi)$.

Equation (12) states that the distances r are equal to scaled values of the function $R_0(\phi)$. This procedure can be used only if amplitudes of all signal components are constant and equal (an assumption made in Section II). Otherwise, distances r can be found directly from the modulus of the AF:

$$\rho_{K/b} = \{\max r : |A_z(r, \phi)| \geq \epsilon |A_z(0, 0)|; \quad \phi \in \Phi_{K/b}\}. \tag{13}$$

Step 3: Kernel generation.

The analytic form of a designed kernel in polar coordinates is given by

$$\varphi(r, \phi) = \begin{cases} 1 & \text{if } \phi \in \Phi_{K/b} \text{ and } r \in \rho_{K/b} \\ 0 & \text{otherwise.} \end{cases} \tag{14}$$

Fig. 6 shows the kernel designed for the signal considered in Figs. 2–5. The parameters used are: $K = 2$ (case 1 in step 1) or $\beta = 0.02$ (case 2 in step 1) and $\epsilon = 0.1$. The resulting time-frequency distribution with eliminated cross-terms and preserved time and frequency resolution is plotted in Fig. 7. For comparison, the short-time spectrogram of the same signal is shown in Fig. 8.

Implementation Notes: In practical implementation of steps 1 and 2, in the transformation from Cartesian to polar coordinates, linear interpolation was used. In step 3, the kernel edges have to be ta-

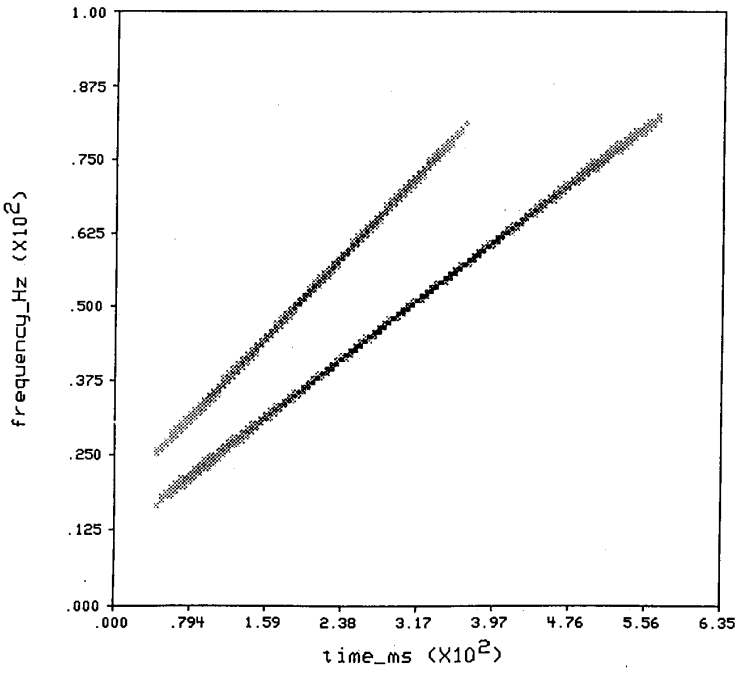

Fig. 7. Resulting time-frequency representation of signal A (cross-terms eliminated, frequency resolution preserved).

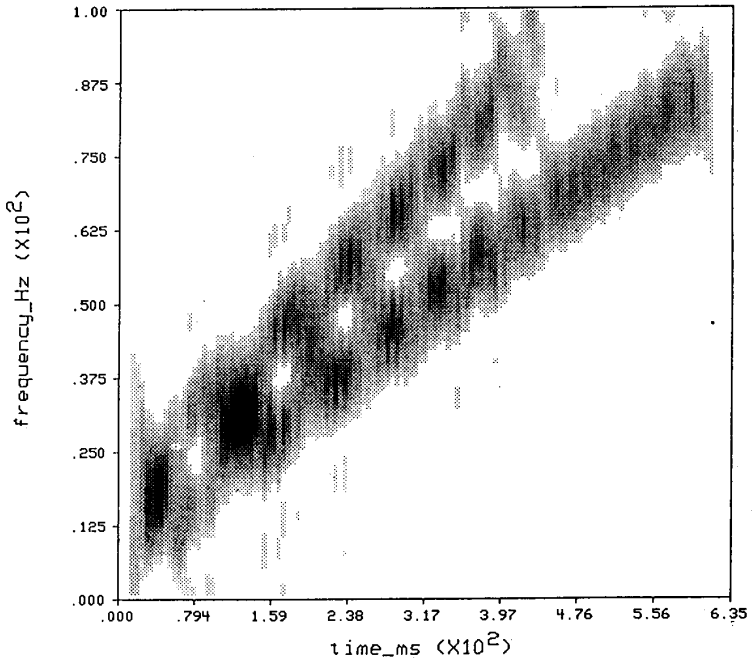

Fig. 8. Short-time spectrogram of signal A.

pered in order to reduce Gibbs phenomena (the sidelobes effect) since the kernel is a 2D filter.

Simulation Result in Noise: Consider the same signal treated in previous examples, embedded in noise such that SNR is 6 dB. Fig. 9 presents the $R_0(\phi)$ function. Observe that two sharp peaks are preserved, but the level is increased almost uniformly due to the noise power. Figs. 10 and 11 show the WVD and the resulting time-frequency representation after 2D filtering, respectively.

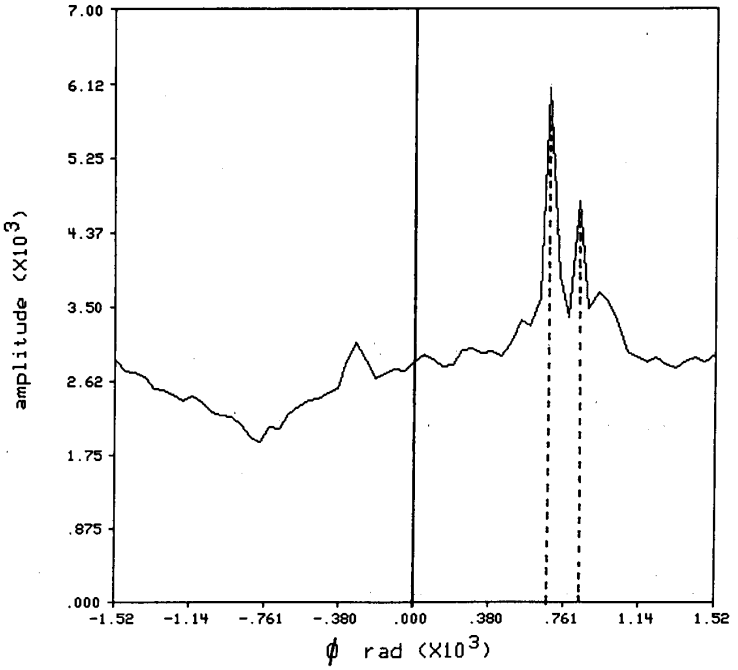

Fig. 9. Radon transform at $s = 0$ of the modulus of the AF of signal A embedded in noise (SNR = 6 dB).

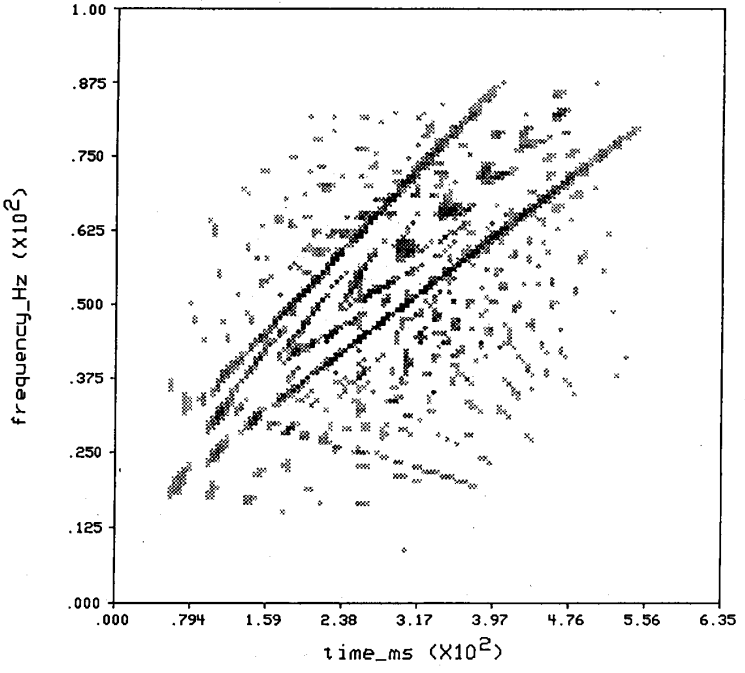

Fig. 10. Wigner–Ville distribution of signal A embedded in noise (SNR = 6 dB).

IV. Nonlinear FM Signal Components

Since a nonlinear FM signal can be considered as a large number of linear FM signals with time-varying frequency rate a_{2k}, the modulus of the AF of a nonlinear FM signal would contain a collection of lines going through the origin with time varying angle ϕ_k. Therefore, the technique proposed in the Section III could be applied even to nonlinear FM signals. The design procedure, in step 1, would assume that an unknown number of linear FM signal com-

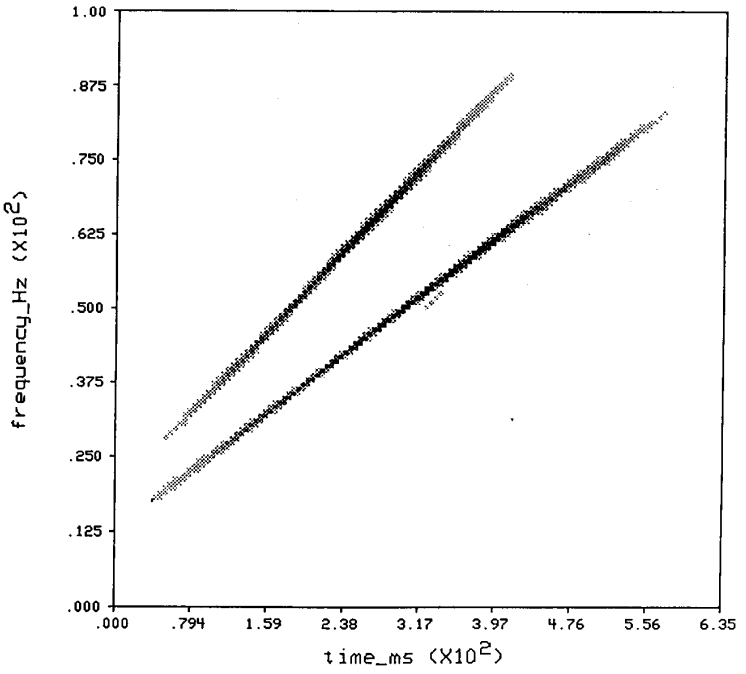

Fig. 11. Resulting time-frequency representation of signal A embedded in noise (SNR = 6 dB).

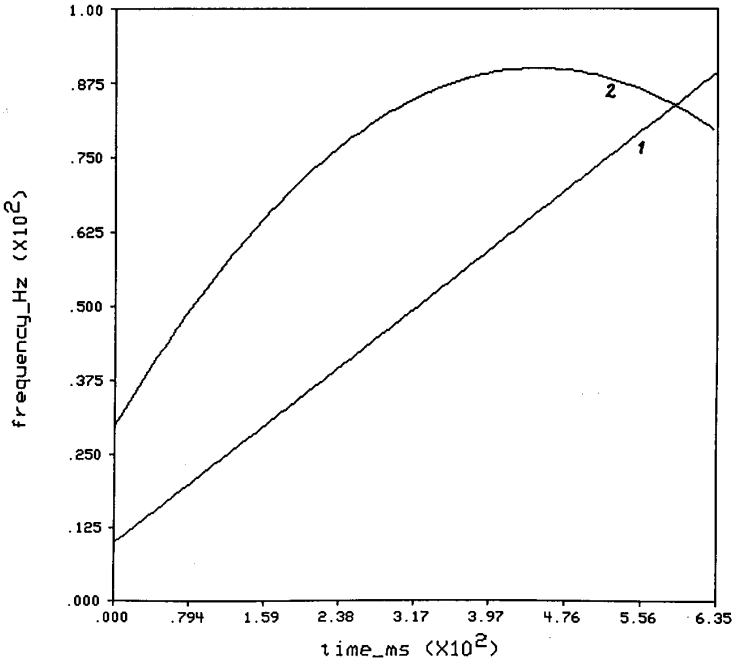

Fig. 12. Instantaneous frequencies of signal B consisting of linear FM and quadratic FM components.

ponents are present in a signal $z(t)$ (case 2). For illustration, a signal consisting of two components, linear and quadratic (their instantaneous frequencies are shown in Fig. 12), is considered in the next example. In Fig. 13, a WVD of the signal is given. The AF of the quadratic component only is presented in Fig. 14. Obviously, there is a range of angles ϕ in which linear FM's are pres-

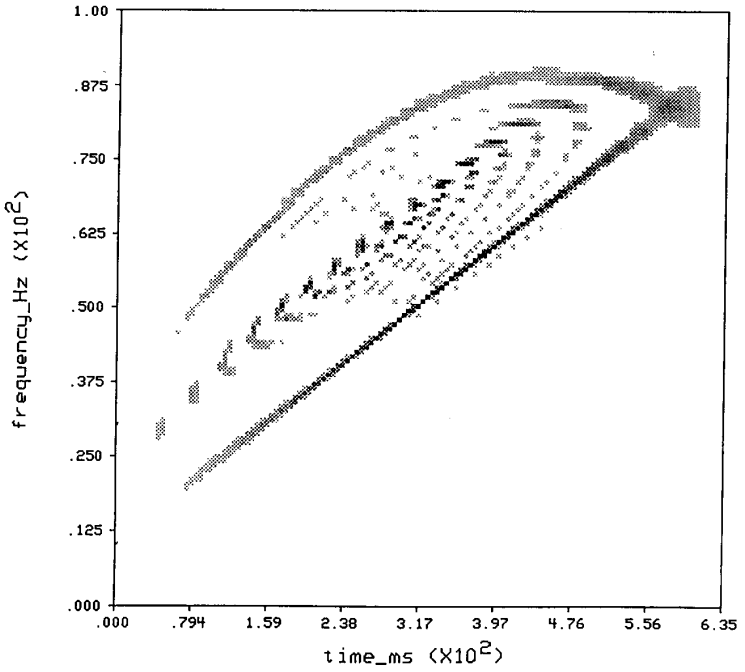

Fig. 13. Wigner–Ville distribution of signal B.

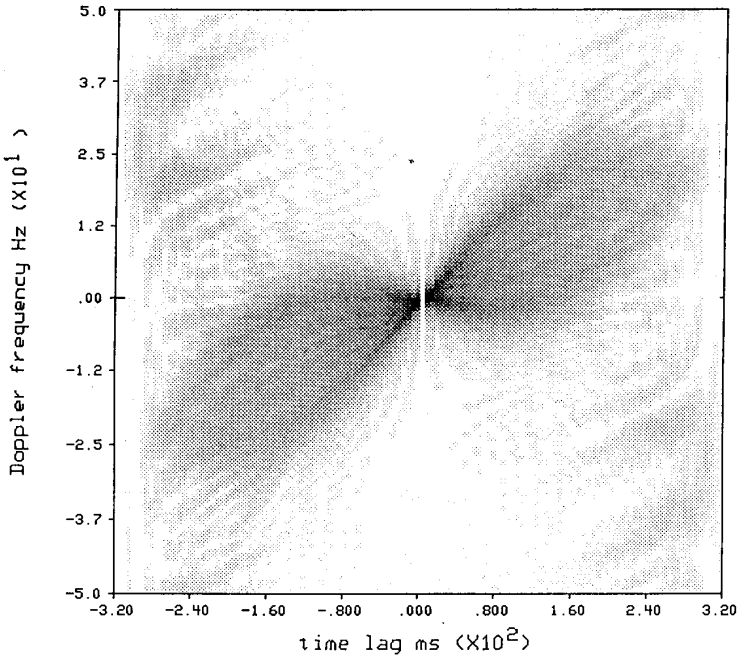

Fig. 14. The modulus of the ambiguity function of the quadratic FM component of signal B.

ent. The AF of the composite signal is shown in Fig. 15. The $R_0(\phi)$ function is plotted in Fig. 16. It indicates where the linear autoterm is by a sharp peak. However, it also shows the range of angles ϕ of the second quadratic component. Figs. 17 and 18 show the designed untapered kernel and the resulting time-frequency representation, respectively (the parameters used are $\beta = 0.09$ and $\epsilon =$

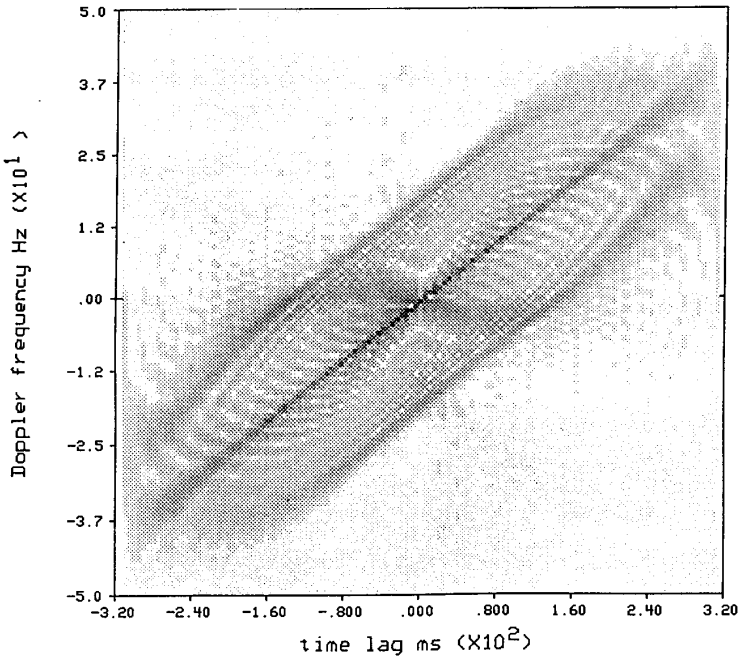

Fig. 15. The modulus of the ambiguity function of signal B.

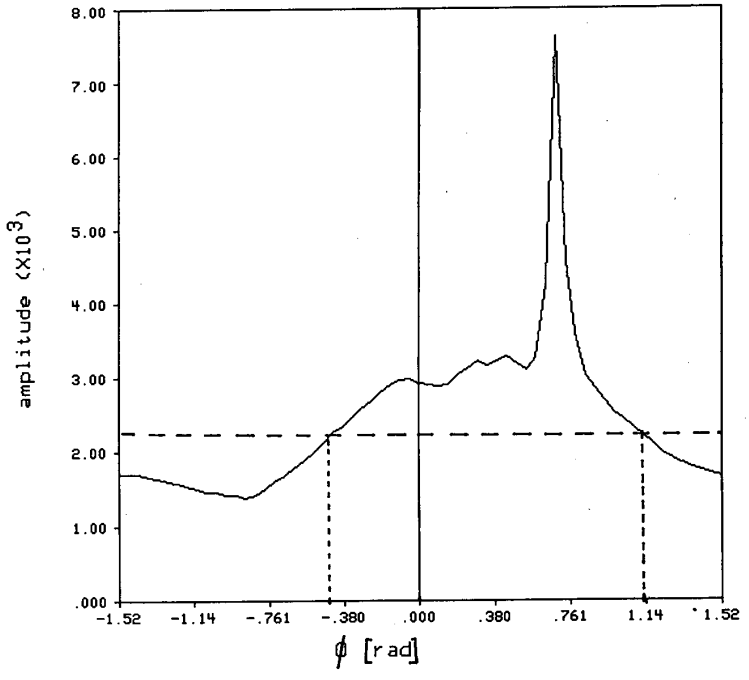

Fig. 16. Radon transform at $s = 0$ of the modulus of the AF of signal B.

0.1). Again, for comparison, in Fig. 19 the short-time spectrogram of the signal is presented. The experiment is repeated for the same composite signal embedded in 6 dB noise. The $R_0(\phi)$ function and the resulting time-frequency representation are shown in Figs. 20 and 21, respectively.

The poorer performance for the case of nonlinear signals comes

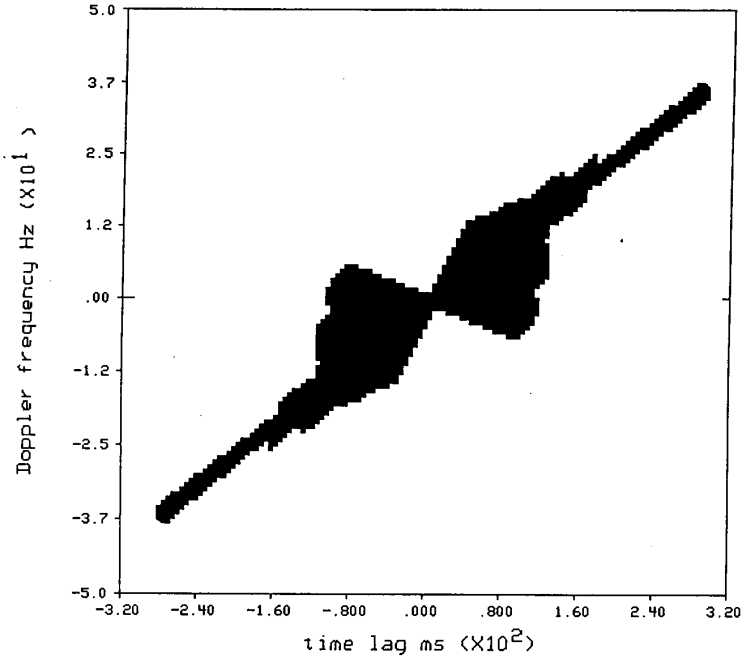

Fig. 17. Kernel designed for signal $B(\beta = 0.09$ and $\epsilon = 0.1)$.

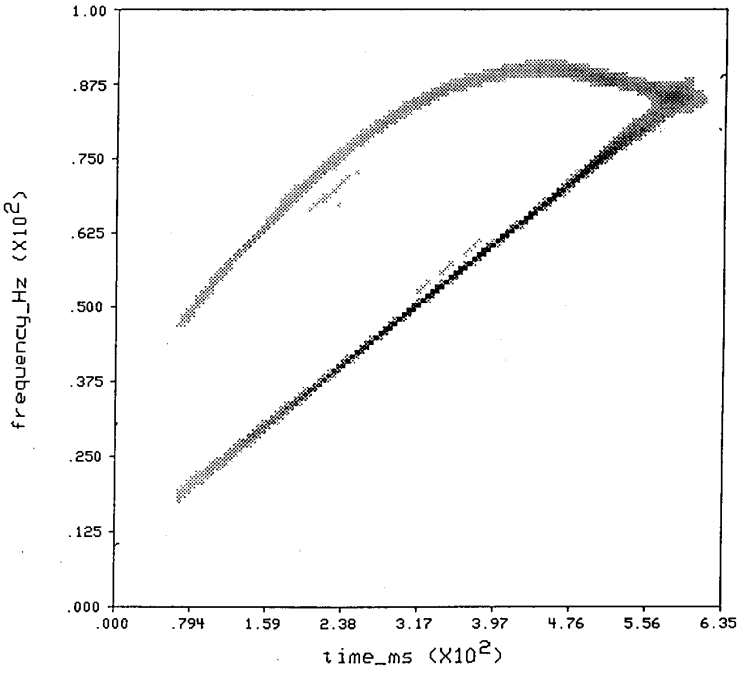

Fig. 18. Resulting time-frequency representation of signal B.

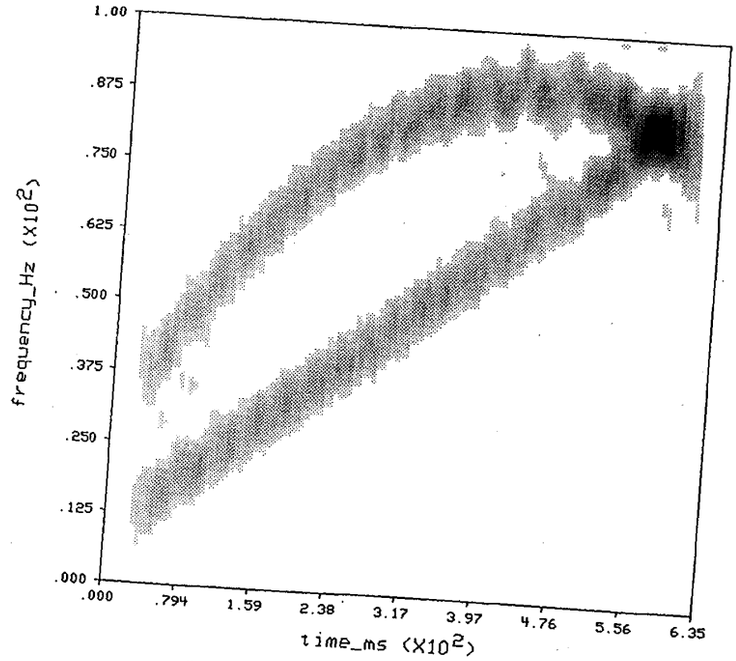

Fig. 19. Short-time spectrogram of signal B.

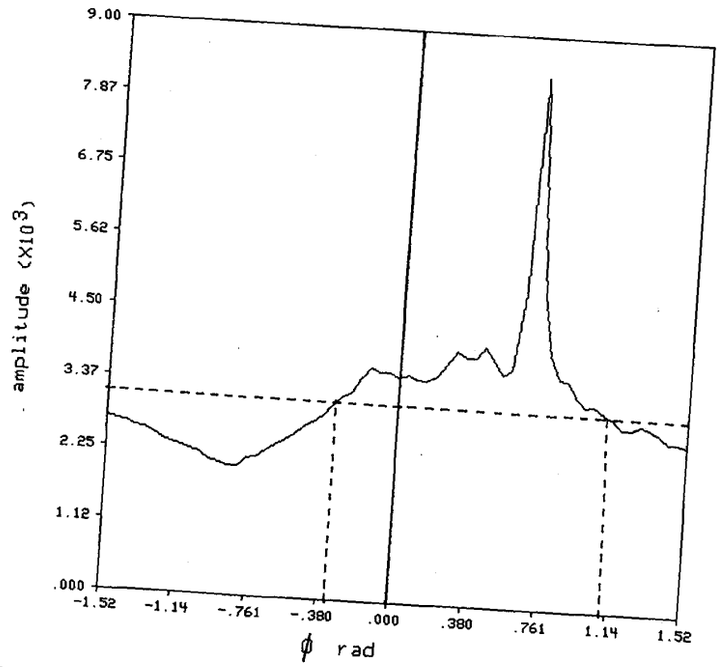

Fig. 20. Radon transform at $s = 0$ of the modulus of the AF of signal B embedded in noise (SNR = 6 dB).

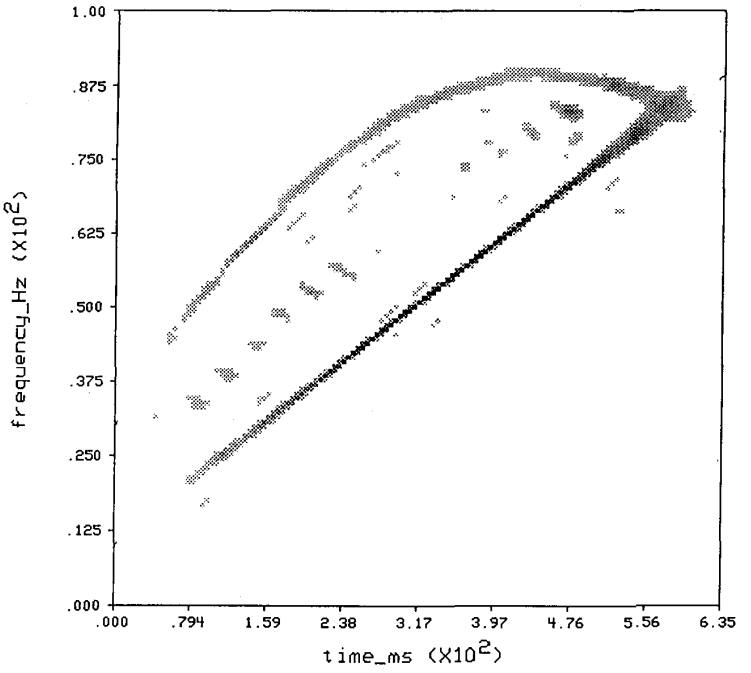

Fig. 21. Resulting time-frequency representation of signal B embedded in noise (SNR = 6 dB).

from the fact that the bilinear time-frequency representations of monocomponent nonlinear FM signals generate what are commonly called "self-cross-terms," and this effect cannot be optimally removed simply by filtering in the ambiguity domain. Thus, for general polynomial FM monocomponent signals one has to use either the multilinear WVD [4] or the Polynomial transform [11]. Adaptive kernel design for these cases is still under investigation.

V. Conclusion

In this correspondence we proposed a new kernel design technique for time frequency analysis which generates TFD's with high frequency and time resolution. The technique is based on the Radon transform applied to the modulus of the ambiguity function of a signal, and is primarily designed for linear FM signal components. Two simulated experiments have shown the robustness of the proposed signal dependent time-frequency representation to noise and cross-terms. It is observed that the kernel can even be applied to nonlinear FM signals with somewhat degraded results.

References

[1] R. G. Baraniuk and D. L. Jones, "A radially Gaussian signal-dependent time-frequency representation," in *Proc. IEEE Int. Conf. Acoust., Speech, Signal Processing.*, Toronto, Canada, May, 1991, pp. 3181–3184.

[2] B. Boashash, "Time-frequency signal analysis," in *Advances in Spectral Estimation and Array Processing*, vol. 1, S. Haykin, Ed. Englewood Cliffs, NJ: Prentice-Hall, 1991, ch. 9, pp. 418–517.

[3] B. Boashash, "Interpreting and estimating the instantaneous frequency of a signal—Part II: Algorithms," *Proc. IEEE*, pp. 539–569, Apr. 1992.

[4] B. Boashash and P. O'Shea, "Time-varying higher order spectra," *Proc. SPIE Int. Soc. Opt. Eng.*, pp. 98–108, July 1991.

[5] I. Choi and W. Williams, "Improved time-frequency representation of multicomponent signals using exponential kernels," *IEEE Trans. Acoust., Speech, Signal Processing*, vol. 37, no. 6, pp. 862–871, June 1989.

[6] T. A. C. M. Classen and W. F. G. Mecklenbrauker, "The Wigner distribution—Part I," *Phillips J. Res.*, vol. 35, pp. 217–250, 1980.

[7] L. Cohen, "Time-frequency distributions—a review," *Proc. IEEE*, vol. 77, no. 7, pp. 941–981, July 1989.

[8] P. Flandrin, "Some features of time-frequency representations of multicomponent signals," in *Proc. IEEE Int. Conf. Acoust., Speech, Signal Processing*, San Diego, CA, 1984, pp. 41B.I.4–41B.4.4.

[9] A. K. Jain, *Fundamentals of Digital Image Processing*. Englewood Cliffs, NJ: Prentice-Hall, 1989.

[10] G. Jones and B. Boashash, "Instantaneous quantities and uncertainty concepts for signal dependent time frequency distribution," *Proc. SPIE Int. Soc. Opt. Eng.*, pp. 167–178, July 1991.

[11] S. Peleg and B. Porat, "Estimation and classification of polynomial phase signals," *IEEE Trans. Inform. Theory*, vol. 37, pp. 422–429, Mar. 1991.

[12] B. Ristic and B. Boashash, "Adaptive time-frequency representations based on the Radon transform," in *Proc. Int. Symp. Signal Processing Its Appl.*, Gold Coast, Australia, Aug. 1992, 41–44.

[13] Y. Zhao, L. E. Atlas, and R. J. Marks, II, "The use of cone-shaped kernels for generalized time-frequency representation of nonstationary signals," *IEEE Trans. Acoust., Speech, Signal Processing*, vol. 38, no. 7, June 1990.

A New Systolic Realization for the Discrete Fourier Transform

Dulal C. Kar and V. V. Bapeswara Rao

***Abstract*—In this correspondence, a new systolic array for the discrete Fourier transform is proposed. In comparison with the earlier schemes, the proposed scheme reduces the number of multipliers re-**

Manuscript received October 1, 1990; revised November 20, 1992. The associate editor coordinating the review of this correspondence and approving it for publication was Dr. John Eldon.

The authors are with The Department of Electrical Engineering, North Dakota State University, Fargo, ND 58105.

IEEE Log Number 9207557.